Angular distributions and mechanisms for light fragment formation in relativistic heavy-ion collisions

J. B. Cumming, P. E. Haustein, and R. W. Stoenner
Chemistry Department, Brookhaven National Laboratory, Upton, New York 11973
(Received 13 November 1985)

Angular distributions are reported for ^{37}Ar and ^{127}Xe produced by the interaction of 8-GeV ^{20}Ne and 25-GeV ^{12}C ions with Au. A shift from a forward to a sideward peaked distribution is observed for ^{37}Ar, similar to that known to occur for incident protons over the same energy interval. Analysis of these data and those for $Z=8$ fragments indicate that reactions leading to heavy fragment emission become more peripheral as bombarding energies increase. A mechanistic analysis is presented which explores the ranges of applicability of several models and the reliability of their predictions to fragmentation reactions induced by both energetic heavy ions and protons.

I. INTRODUCTION

Although copious ejection of light fragments ($A \lesssim 50$) from medium- and heavy-mass targets was one of the first new phenomena observed after multi-GeV protons became available about 30 years ago,[1] the mechanism responsible for their production remains unclear. Measurements of particle multiplicities associated with fragments show that very violent interactions and a multibody final state are involved.[2] There is no agreement, however, on whether the observed fragments have their origin in regions of highly excited nuclear matter or represent relatively undisturbed remnants of the target nucleus. The topic has been the subject of recent reviews.[3,4]

Observations by the Purdue-Fermilab[5,6] group of an approximate power law dependence of inclusive cross sections on fragment mass have provided impetus for attempts[7,8] to analyze a wide range of data in terms of models involving phase instabilities during the expansion of extended regions of hot nuclear matter (~ 100 nucleons). A power law is expected if the system is near the critical point of nuclear matter at final freeze-out. However, simulations based on the expansion of hot classical drops suggest[9] that heavy aggregates do not arise from such trajectories, but rather from those which enter the adiabatic spinodal zone, well below the critical temperature. A quantum statistical treatment of hot nuclear matter[10] appears to be able to account for the yields of target rapidity fragments without involving phase instabilities.

In general, such "hot" models focus on the decay of essentially equilibrated systems but not on how or if such systems are formed in the initial projectile-target interaction. Considerable detail of the initial step is provided by a hydrodynamical calculation[11] of heavy-ion interactions which identifies fragment precursors with cold spectator parts of the target. For the system 8-GeV ^{20}Ne + U, side splash and projectile bounce off lead to substantial transverse momentum transfer to fragments. In the cold cleavage model,[12] details of the initial interaction were adjusted in an *ad hoc* fashion to account for observed energy and angular distributions of Sc fragments from 400-GeV proton interactions with U.[13]

An interesting and unexpected feature of proton-induced fragmentation is the development of sideward peaked angular distributions at energies above ~ 10 GeV.[14,15] In the limiting fragmentation region ($E \gtrsim 20$ GeV), intensities of some species at 0° become lower than those at 180°.[16,17] Such phenomena have not been reported for heavy-ion projectiles. However, angular distributions of $Z=8$ fragments formed in ^{20}Ne interactions with Au hinted that sideward emission might be observed above Bevalac energies.[2] Based on systematics of proton-induced reactions it was thought that sideward peaking might be pronounced for species heavier than $Z=8$, even at 2 GeV/nucleon. However, previous attempts[18] to measure angular distributions of such heavier fragments by radiochemical techniques gave marginal results due to low beam intensities.

The present experiment was initiated to obtain reliable angular distributions of some heavy fragments from the interaction of 8-GeV ^{20}Ne and 25-GeV ^{12}C with Au. These kinetic energies span the onset of sideward peaking in proton-induced reactions. The choice of Au as a target avoids experimental complications from the large fission cross section of U. A variety of other experimental data is also available for protons[19] and heavy ions[20] incident on Au. Techniques developed for the assay of lunar samples[21] were employed to assay the low levels of activity. Two products representing interesting mass regions are amenable to such procedures: ^{37}Ar, a typical heavier light fragment of the sort known to show sideward peaking in proton-induced reactions;[15] and ^{127}Xe, representative of deep spallation. Counter data[2] indicate no appreciable contribution of binary events to either product at the energies of interest. A preliminary report of results for 25-GeV ^{12}C ions has been published.[22]

II. EXPERIMENTAL PROCEDURES

This experiment utilized an evacuated cylindrical scattering chamber (38.6-cm long, 19.7-cm diam). A beam of 8-GeV ^{20}Ne or 25-GeV ^{12}C ions from the LBL

 ©1986 The American Physical Society

Bevalac passed along the axis of the cylinder, entering and exiting through 6.1-cm diam Mylar windows. Fragments recoiling from a 200-μg/cm^2 Au foil inclined at a 45° angle at the chamber center were stopped in two layers of 21-mg/cm^2 Al which lined the chamber except for the window areas. For increased strength, targets were supported on 60-μg/cm^2 Formvar backings.

The 200-μg/cm^2 thickness represented a compromise: sufficiently thin to avoid major distortions of angular distributions due to scattering or absorption yet thick enough to give activity levels which could be measured reliably. Thick-target, thick-catcher data[20] indicate that only $\sim$4% of the produced ^{127}Xe and $\sim$1% of the ^{37}Ar would be retained in such a target. Because azimuthal angles of the catcher foils in the present experiment were selected so that mean recoil paths in the target were $\leq$150 μg/cm^2, still smaller effects were anticipated. The following auxiliary measurements with 25-GeV ^{12}C ions confirmed this: increasing the mean path traversed at 54° from 125 to 295 μg/cm^2 resulted in 2$\pm$6% and 3$\pm$4% decreases in intensity of ^{37}Ar and ^{127}Xe fragments; and including Formvar in the recoil path at 90° gave an apparent increase of ^{37}Ar by 7$\pm$8% and a decrease of ^{127}Xe by 1$\pm$4%. Recoils collected over 1.65π sr were therefore not significantly affected by scattering or absorption. Similar checks were not included in the 8-GeV ^{20}Ne experiment. However, the target was reversed so lower-energy, backward-moving recoils did not traverse the Formvar.

Each irradiation was $\sim$30 h in duration, and fluences of 4.4×10^{13} ^{12}C ions and 3.8×10^{13} ^{20}Ne ions were determined from ^{127}Xe production in downstream Au monitor foils. Relative to the 17.1$\pm$2.7 mb cross section reported[20] for ^{127}Xe production by 25-GeV ^{12}C and the 11.5$\pm$1.4 mb by 8-GeV ^{20}Ne, the ^{37}Ar cross sections were found to be 6.6$\pm$1.0 and 3.9$\pm$0.5 mb, respectively.

After irradiation, catcher assemblies were returned to Brookhaven National Laboratory (BNL) where they were cut into nine 18° sectors covering angles from $\theta_{lab}=9°$ to 171°. As noted above, azimuthal angles of each sector were limited to avoid long recoil paths in the target. One 21-mg/cm^2 Al foil is sufficiently thick to stop recoils with energies up to 7 MeV/nucleon and no significant ^{37}Ar or ^{127}Xe was detected in the second layer of foil which lined the cylindrical body of the scattering chamber. Some ^{37}Ar, but no ^{127}Xe, was found in the second foils positioned nearer to the beam on the inside of the chamber end caps (9°–27° and 153°–171°). This was ascribed to ^{37}Ar production by beam halo interacting with the $\sim$70 ppm of impurities in the Al. As a percentage of the activity in the primary catchers, these blanks amounted to 12% at 18° and 7% at 162° for incident ^{12}C ions, and 7% and 14% at the same angles for ^{20}Ne.

Procedures for the assay of ^{37}Ar and ^{127}Xe were modified from those developed for the assay of the low levels of radioactivity encountered in lunar samples.[21] Each foil was vacuum melted in the presence of Ar, Kr, and Xe carriers, and the noble gases were separated chromatographically on charcoal columns using He as a carrier. After cleanup over hot V, the Ar and Xe fractions were transferred with added P-10 gas into small proportional counters. Earliest assays started $\sim$5 d after the end of irradiation and continued for $\sim$six months. Pulse spectra were acquired with several multichannel analyzers at 256 channel resolution. After visual inspection of the spectra to ascertain that the counting systems were functioning properly, data for seven relevant regions of interest were recorded for subsequent analysis. While not all samples were counted for the full period, sufficient data were acquired to examine decay and background effects in detail. Since the same set of counters was used for both ^{12}C and ^{20}Ne experiments, consistency checks on backgrounds were possible. As anticipated, 36.4-d ^{127}Xe and 35.1-d ^{37}Ar were the only long-lived products observed. Had a U target been used, the Xe decay would have been considerably more complex.[23] Counting rates varied from $\sim$30 to $\sim$300/d, depending on the sample. Background rates were $\approx$1–3/d. ^{127}Xe was assayed with an efficiency of $\sim$70% with an energy window encompassing the K and L Auger and conversion electron peaks. ^{37}Ar was assayed with a window on the K Auger peak which resulted in efficiencies of $\sim$54%. End-of-irradiation activities were obtained by least squares analysis of the decay curves. Corrections were applied for chemical yields on the basis of recovered gas volumes, for counting efficiencies determined for each counter using standardized ^{37}Ar and ^{127}Xe samples, and for the ^{37}Ar blanks at 18° and 162°. Single differential cross sections $(4\pi/\sigma)(\delta\sigma/\delta\Omega)$ were then obtained from the production rates and solid angles subtended by each sector. These "raw" values were corrected for experimental resolution by the following iterative procedure. A least-squares fit of the raw data to a power series in $\cos\theta$ provided an initial approximation of the true angular distribution. This served as input for a program which calculated what would have been observed for the actual catcher areas. Resolution corrections were then computed at each angle. These were applied to the raw data to obtain a better approximation, and the cycle repeated. Corrections were found to be unchanged after the second iteration. Resolution corrections were largest for the most anisotropic distribution (^{127}Xe at 8 GeV) but they never exceeded 9%.

III. RESULTS

Normalized angular distributions for ^{37}Ar and ^{127}Xe are shown in Fig. 1. Error bars include uncertainties from counting statistics, chemical yields, and counter efficiencies. Those for ^{37}Ar include an assumed 50% error in the blank corrections which were applied at 18° and 162°. Figure 1 also shows angular distributions for $Z=8$ fragments produced by 8-, 21-, and 42-GeV ^{20}Ne ions incident on Au.[2] Smooth curves in Fig. 1 are least-squares fits to the function

$$f(\theta)=a_0+a_1\cos\theta+a_2\cos^2\theta+a_3\cos^3\theta\ . \quad (1)$$

The quality of the fits was consistent with $a_3=0$ for ^{37}Ar and $Z=8$. A cubic term was required to satisfactorily describe the distributions of ^{127}Xe. In all fits, the a_0 term is forced by the data normalization to be equal to $1-a_2/3$.

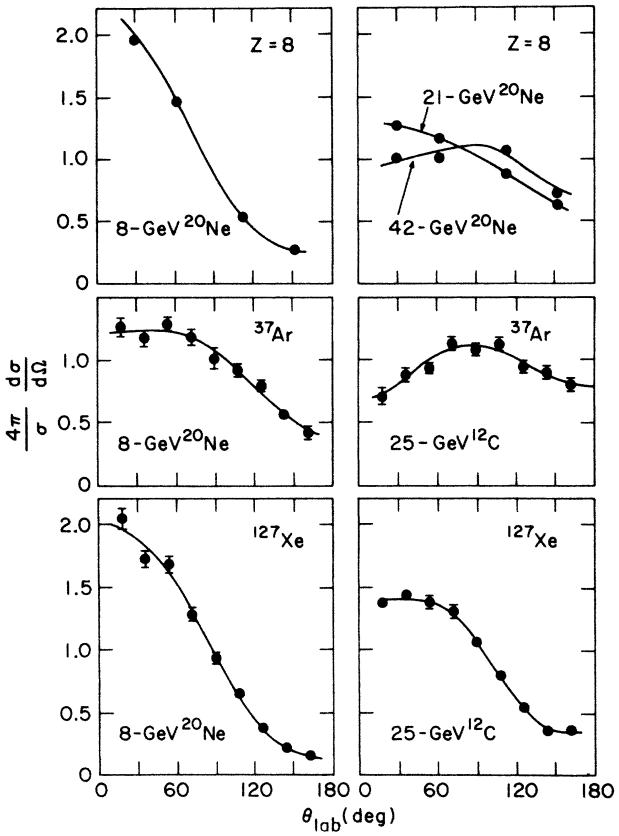

FIG. 1. Angular distributions of $Z=8$, ^{37}Ar, and ^{127}Xe fragments from the interactions of the indicated projectiles with Au. Those for ^{37}Ar and ^{127}Xe are from the present experiment, those for $Z=8$ from Ref. 2.

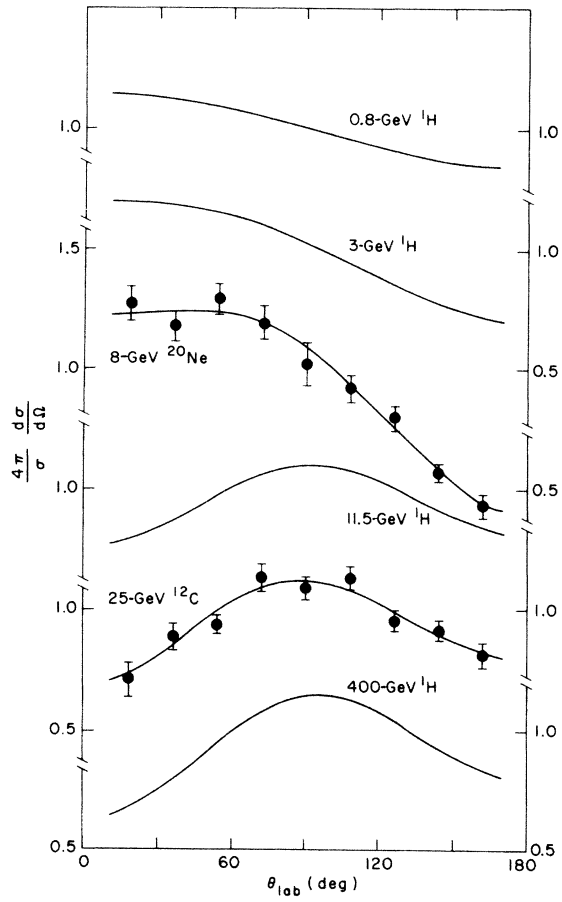

FIG. 2. Comparison of angular distributions for ^{37}Ar produced in heavy ion interactions with those for similar products in proton bombardments. Points are from the present experiment. Curves without points are based on data from Ref. 15 for scandium isotopes.

In discussing the change of the angular distribution from strongly forward peaked (the forward to backward ratio $F/B=3.3\pm0.3$) for 5-GeV ^{20}Ne ions (not shown in Fig. 1) to approaching isotropy ($F/B=1.14\pm0.09$) at 42 GeV, Warwick *et al.*[2] concluded that sideward peaking might be observed for $Z=8$ fragments at still higher energies. While the curve for $Z=8$ in Fig. 1 suggests some sideward preference at 42 GeV, the present results for ^{37}Ar production by 25-GeV ^{12}C ions provide the first definitive evidence for this effect in reactions induced by relativistic heavy ions.

Angular distributions of all three products shift forward as the beam energy decreases from 25 to 8 GeV. For ^{37}Ar, F/B increases from 0.98 ± 0.02 to 1.52 ± 0.04 and for ^{127}Xe from 2.02 ± 0.04 to 3.05 ± 0.11. Sideward peaking is no longer apparent for ^{37}Ar at 8 GeV, although the distribution is relatively flat at forward angles.

The present results for ^{37}Ar are compared in Fig. 2 with angular distributions[15] of Sc isotopes produced in 0.8- to 400-GeV proton interactions with U. The shape of the ^{37}Ar curve for incident 25-GeV ^{12}C ions, including lower intensities at 0° compared to 180°, is essentially identical to that observed for protons of the same kinetic energy. Sideward peaking also disappears over the same general energy interval, but the angular distribution of ^{37}Ar produced by 8-GeV ^{20}Ne is significantly more forward peaked than those produced by protons of any energy.

Parameters from fits of angular distributions to Eq. (1) facilitate a more quantitative comparison of data for different projectiles and energies. The quantity $a_1/2$ is a measure of the forward shift of an angular distribution and is equal to $F-B$, the excess of fragments in the forward hemisphere. The anisotropy coefficient a_2 leads to enhanced or suppressed emission at 90° depending on its sign. The fragment mass dependence of these parameters at a fixed projectile energy is examined in Fig. 3. The curves in this figure are determined by the extensive data for 28-GeV protons incident on Au shown as small points.[14,17,24] Sideward peaking was first observed in a counter study of $Z=6$ to 13 fragments.[14] An activation technique provides data for fragments from ^{24}Na to ^{149}Gd.[17] For protons incident on Au, sideward peaking is observed for a broad range of masses from $A\sim15$ to $A\sim95$ where small or slightly negative values of $a_1/2$

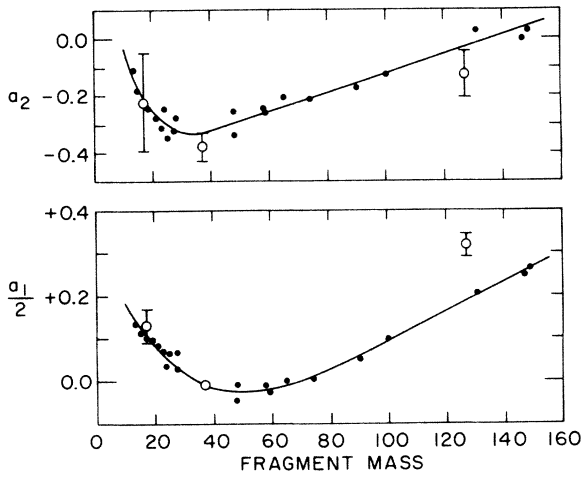

FIG. 3. Dependence of parameters of angular distributions on fragment mass. Open points are from the present work and Ref. 2 for ~25-GeV heavy ion interactions with Au. Small closed points are for proton induced reactions from Refs. 14, 17, and 24. Solid curves show general trends.

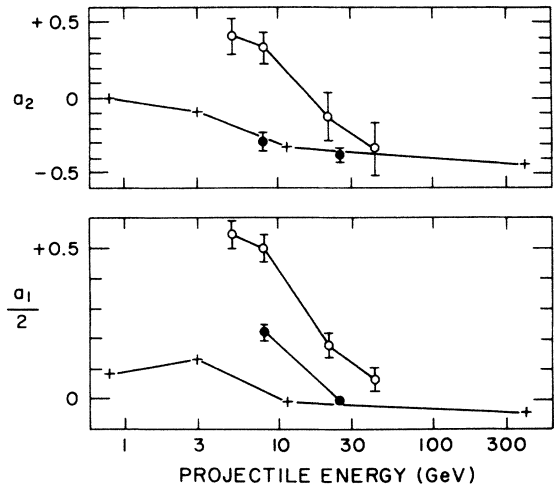

FIG. 4. Projectile energy dependence of angular distribution parameters in proton and heavy-ion induced fragmentation: (○), $Z=8$ fragments from ^{20}Ne interactions with Au, Ref. 2; (●) ^{37}Ar from the present work; (+) scandium fragments from proton interactions with U, Ref. 15.

occur in combination with significantly negative values of a_2. For protons incident on U, angular distributions for $A \lesssim 60$ fragments are similar to those from Au, but the right-hand ascending branches of the curves in Fig. 3 are shifted to higher masses. Values of a_2 comparable to those at the minimum persist even in the $A \sim 131$ region.[25] Figure 3 shows that results for $Z=8$ and ^{37}Ar produced in heavy-ion interactions track the proton data very closely. (Parameters for $Z=8$ were interpolated between the 21 and 42 GeV results.)

The energy dependence of angular distribution parameters for light fragments produced in heavy-ion interactions is examined in Fig. 4. Baseline data are results for Sc isotopes produced by incident protons[15] which show that the forward shift $a_1/2$ reaches a maximum at ~3 GeV and then falls to slightly negative values in the limiting fragmentation region. A maximum in the 2–3 GeV region is confirmed by F/B ratios from thick-target, thick-catcher experiments.[19] The rapid decrease of a_2 and $a_1/2$ between 3 and 11.5 GeV makes the onset of sideward peaking apparent in this region.

Parameters for both ^{37}Ar and $Z=8$ appear to approach limiting conditions defined by the Sc results as the projectile energy increases. Figure 4 confirms the surmise[2] that angular distributions of $Z=8$ fragments will become sideward peaked at energies above 42 GeV. The anisotropy a_2 at that energy is already comparable to those of the sideward peaked ^{37}Ar and Sc fragments, but $a_1/2$ is still decreasing. With decreasing energy, ^{37}Ar and $Z=8$ diverge from each other and from the comparison proton induced reaction. The a_2 for ^{37}Ar at 8 GeV, however, remains comparable to that for protons. Disappearance of the sideward peak is due to a more rapid rise of $a_1/2$. There is the suggestion in Fig. 4 that differences in angular distributions between $Z=8$ and ^{37}Ar will disappear above 42 GeV. However, at ~25 GeV a significant dependence on fragment mass over the region $A=15$ to $A=45$ remains.

The present results confirm that neither projectile energy nor rapidity is a satisfactory scaling variable for products far removed from heavy element targets.[26] For reactions involving smaller mass losses from Cu targets, kinetic properties are essentially independent of projectile mass if comparisons are made at the same rapidity.[27] It is apparent in Fig. 2 that the angular distribution of ^{37}Ar for 2.1-GeV/nucleon ^{12}C is grossly different from that which would be observed for 2.1-GeV protons but the same as that for 25-GeV protons. On the other hand, it appears that no energy proton will give an ^{37}Ar distribution as forward peaked as that observed for 8-GeV ^{20}Ne. The angular distribution of ^{127}Xe produced by 25-GeV ^{12}C ions is also appreciably more forward peaked (Fig.3) than that expected for the same energy protons.

IV. DISCUSSION

A. Overview

A general picture of the interactions that lead to target-rapidity fragment production in heavy-ion interactions can be drawn from counter and streamer chamber studies. Data of Warwick *et al.*[2] show the multiparticle nature of the final state: ~6 fragments with $2 \lesssim Z \lesssim 27$ are associated with each $A=20$–40 fragment detected at 90°. The mass distribution of the associated fragments is the same as that of the inclusive cross sections. While multiplicity measurements show that fragment production is associated with very violent collisions, Gutbrod *et al.*[28] have pointed out an important change with bombarding energy. For energies up to 8 GeV, the same multiplicities are associated with proton and fragment triggers. Above this energy, the multiplicity associated with fragments

TABLE I. Parameters derived from angular distributions of fragments from the interaction of heavy ions with gold.

Fragment, projectile, and energy (GeV)		η Expt.	θ (deg) Expt.	θ (deg) Calc.[a]	$10^3\,\beta$ Expt.	$10^3\,\beta$ Calc.[a]
$Z=8$, ^{20}Ne,	5	0.55±0.05	0±6		45 ±4	
	8	0.50±0.05	1±6	84	43 ±5	55
	21	0.50±0.15	69±9		42 +13	
	42	0.51±0.16	82±4		42 +13	
^{37}Ar, ^{20}Ne,	8	0.71±0.04	73±1	83	30 ±2	43
^{12}C,	25	0.68±0.03	91±1		28 +1	
^{127}Xe, ^{20}Ne,	8	0.76±0.02	48±2	90	8.5±0.2	11
^{12}C,	25	0.68±0.05	62±3		7.5±0.6	

[a]From Ref. 11. Precursors for $Z=8$, ^{37}Ar, and ^{127}Xe were assumed to be $A=24$, 44, and 148, respectively.

rises less rapidly than that associated with proton triggers. By 42 GeV it is 50% lower. Evidently the most violent, and presumably most central, collisions above 8 GeV no longer lead to mass 20—40 emission. Renfordt *et al.*[29] have concluded from exclusive charged particle data for ^{40}Ar + Pb at 31 GeV that there is sideward flow in the case of semicentral collisions ($3 \leq b \leq 5.5$ fm), whereas central collisions result in complete stopping in the participant center of mass. It is attractive to relate these observations to the changes in $Z=8$ and ^{37}Ar angular distributions with energy. At 8 GeV, projectile stopping results in forward momentum transfer to the prefragment system and ultimately in forward peaked fragment distributions. As the energy increases the reactions selected by fragment survival became increasingly peripheral, and the direction of momentum transfer shifts from forward to sideward.

To examine this idea quantitatively, we invoke a two-step model in which the initial projectile-target interaction results in an excited prefragment moving with a speed v at an angle θ in the laboratory system. Subsequent breakup of this precursor adds an additional, assumed isotropic velocity V, e.g., by acceleration of the separating fragments in the Coulomb field. In this picture the shape of an angular distribution is determined by the ratio $\eta=\langle v/V\rangle$ and the angle θ. The forward component of η, $\eta_{||}$, is equal to $F-B$. If the perpendicular component $\eta_{\perp}$ is sufficiently large, sideward peaking will be observed. It should be pointed out that an alternative interpretation of sideward peaking is an intrinsic anisotropy of the deexcitation process. For example, angular momentum effects in binary fission may give sideward peaked distributions.[30] Since experimental results[2] indicate, at most, small contributions of binary processes to the species examined in the present work, we emphasize the directed momentum transfer picture.

An iterative nonlinear least squares procedure was used to obtain values of η and θ for the $Z=8$, ^{37}Ar, and ^{127}Xe angular distributions. Results of this analysis given in Table I show the expected shift in direction of first step momentum transfer to more sideward emission at high bombarding energies. Changes in angular distributions are the result of this shift: η is essentially energy independent for a given product. It is significant that momentum imparted during the breakup of prefragments shows essentially no dependence on projectile type and only a weak dependence on bombarding energy. Values of $P=AV$ for ^{37}Ar and ^{127}Xe in Fig. 5, were obtained by interpolation between those for similar products measured by the thick-target, thick-catcher technique.[19,20] Those for $Z=8$ fragments were obtained from energy spectra.[2,24] Evidently the intermediate systems which give rise to a particular fragment are very similar in proton and heavy-ion interactions.

Combination of values of V with those for η leads to estimates which are given in Table I of the velocity $\beta=v/c$ of the prefragment after the first reaction step. This analysis resolves what, on first sight, is a paradox in the experimental data: angular distributions of ^{127}Xe are

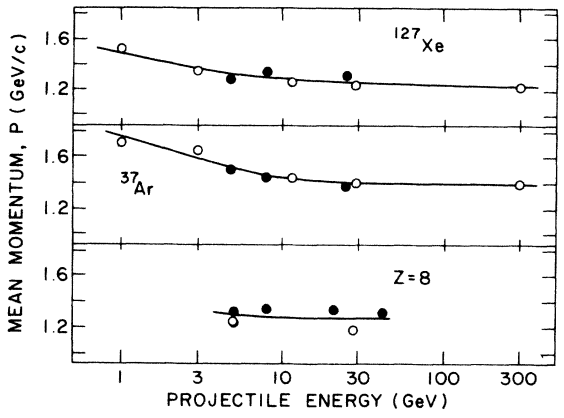

FIG. 5. Dependence of mean momentum imparted during the second or breakup step of reactions leading to ^{127}Xe, ^{37}Ar, and $Z=8$ fragments on projectile type and energy. Open points are for incident protons and ^{4}He, closed ones for ^{12}C and ^{20}Ne. Points for ^{127}Xe and ^{37}Ar were interpolated between the data of Refs. 19 and 20. Those for $Z=8$ fragments are from spectra reported in Refs. 2 and 24.

more forward peaked than those of ^{37}Ar despite the fact that the multiplicity associated with ^{127}Xe formation is only about half that associated with ^{37}Ar. Values of β in Table I confirm that ^{127}Xe is formed in less violent events. Its more forward peaked angular distributions at both energies result from a much smaller V combined with the slightly smaller values of θ.

Changes in the direction of β for $Z=8$ fragments are qualitatively in the direction inferred by Gutbrod *et al.*[28] However, if central collisions are involved at energies up to 8 GeV, momentum transfer deduced from angular distributions is too low. Complete transfer would give $\beta=0.070$ at 5 GeV and 0.091 at 8 GeV. The heated and compressed region comprising projectile and participating target nucleons must escape from the spectator regions where fragments will originate before complete energy and momentum sharing can be achieved. This suggests the ideas of "hole boring" and "friction" of the escaping participants as applied by Hüfner *et al.*[12] to account for fragment energy and angular distributions from 400-GeV proton interactions. It seems unlikely that the geometry of the initial interactions of energetic heavy ions and protons would be the same, while as discussed above, the kinetic properties become independent of projectile size at very high energies. It has been suggested by Raha *et al.*[31] that formation of a quark-gluon plasma (QGP) in heavy ion interactions at very high energies would lead to a reduction in the "friction" of the exiting participants and a lower temperature of the spectator matter. Because fragment formation, at least for $Z \geq 8$, has already become peripheral by $2A$ GeV and small momentum transfers are involved, it seems unlikely that measurements of fragments will be a significant test of QGP formation.

B. Hydrodynamical calculations

A detailed calculation of fragment formation in the system 8-GeV ^{20}Ne + U has been performed using a hydrodynamical model in which fragments are considered to originate from regions of the target which remain quasibound after the initial interaction.[11] This calculation predicts a strong correlation between impact parameter and residue mass, extending from $b=4$ fm for $A=24$ to $b=9$ fm for $A=148$. For these impact parameters, side splash and projectile bounce off result in substantial transverse momentum transfer to the residues. The magnitude and direction of the predicted recoil velocities are compared with those deduced from the angular distributions in Table I. Considering uncertainties in both the calculation and in the analysis of the data, the agreement between values of β is good. However, there are problems in the direction of the predicted momentum transfer. It has been concluded[32] that the viscosity assumed in this calculation is a factor of 2 too low. While an increased viscosity would move the direction of momentum transfers to more forward angles, it is not clear that the observed change between $Z=8$ and ^{37}Ar would be quantitatively reproduced. The discrepancy for ^{127}Xe may indicate that the hydrodynamic assumptions are not valid at large impact parameters where projectile-target overlap is small.[11] The calculation in its present form also produces only one heavy residue per interaction rather than the known multibody final state. Since the residues are both distorted and excited, it is possible that they will further fragment to give observed products.

C. Validity of droplet models

An important feature of various droplet models of fragment formation is their focus on the decay of excited intermediates or prefragments. A key assumption is that fragments observed in some mass range arise from fluctuations and instabilities during the expansion and cooling down of prefragments having well-defined nucleon number, volume, and energy/nucleon (or limited ranges thereof). High-energy projectile-target interactions quite clearly can lead to a wide range of prefragment masses and excitations. Furthermore, since multifragmentation appears to involve energy inputs comparable to total binding energies of nuclei,[9,10] more energy efficient pathways, e.g., fission or evaporation from local hot spots, may compete at lower bombarding energies. It is germaine then to question whether an observed distribution of inclusive cross sections is determined by some distribution of prefragments and contributions from several mechanisms or whether it can be related to properties of a nuclear liquid-gas system, such as its critical temperature[8] or degree of saturation.[7]

The angular distribution data discussed above and results from thick-target, thick-catcher recoil studies[19,20] suggest significant changes in mechanism in going from $A=12$ to $A \approx 50$ fragments for both heavy ions and protons with energies of ~ 25 GeV incident on Au. As seen in Fig. 4, the differences between $Z=8$ and $Z=18$ fragments appear to become larger for 8-GeV ^{20}Ne projectiles. Such observations suggest caution in applying the droplet model to such systems.

A striking example of the pitfalls which can be encountered in analysis of inclusive cross sections without examination of other fragment properties can be found in a droplet model treatment[7] of the results for 180- and 360-MeV ^{12}C interactions with Au.[33] Cross sections for $4 \leq Z \leq 26$ spanning two orders could be fit by the model, and a minimum yield for $Z \approx 12$ fragments was taken as evidence for droplet formation in a supersaturated vapor. However, energy and angular distributions[33] strongly suggest the minimum is associated with a change in mechanism. Properties of $Z=5-10$ fragments are well described by assuming that they are emitted from localized regions of high excitation which are in the process of equilibration with the surrounding cold nuclear matter. While angular distributions for $Z \leq 10$ are forward peaked in the center of mass, those for $Z \geq 11$ approach symmetry about 90° and exhibit a $(\sin\theta)^{-1}$ distribution suggestive of fission of a long-lived composite system at high angular momentum.

The question of time scale for multifragmentation is also of considerable importance. The analysis of angular distributions described above (Table I) assumed there was sufficient time between the initial projectile-target interaction and the subsequent breakup for shape distortions and

TABLE II. Forward velocities of systems emitting $Z=8$ fragments in the interaction of ^{20}Ne with gold as inferred from angular distributions and energy spectra.

^{20}Ne energy (GeV)	$10^3\ \beta_{\|\|}$ Angular distribution[a]	Spectra[b]
5	45±4	18±1
8	43+4	14+3
21	15±3	9±2
42	6±3	6+2

[a]From the present analysis of the data of Ref. 2.
[b]Reported in Ref. 2 for $8 \leq Z \leq 11$ fragments.

local hot spots in the prefragments to relax to the equilibrium conditions postulated in droplet and quantum statistical treatments. If that is the case, values of $\beta_{\|}=\beta\cos\theta$ inferred from angular distributions should be the same as those obtained from the shifts of energy spectra with angle of observation.[2] As can be seen in Table II, there are more fragments in the forward hemisphere at low bombarding energy than expected from momentum focusing due to the forward motion of the emitting system. Such differences are well known for incident protons[34–36] where they are interpreted as evidence that the fragmentation is rapid. (Passage of a relativistic projectile across the diameter of a Au nucleus sets a time scale of ~ 13 fm/c.) The apparent agreement in values of $\beta_{\|}$ at 42 GeV is believed to represent a crossover. If the trends shown in Fig. 4 continue, properties of $Z=8$ fragments at higher energies should approach those of Sc isotopes from U. A detailed analysis of that system also indicates a failure of the two-step model, but too many fragments appear in the backward hemisphere at 400 GeV.[36] The present results, in combination with evidence[20] of a forward directed $v_{\|}$ also suggest excess backward emission for ^{37}Ar at 25 GeV. If fragment formation is a rapid process, sufficient time may not be available for the attainment of equilibrium configurations which are the starting point for the phase transition or quantum statistical treatments.

V. CONCLUSIONS

Although fragment formation has been studied for some 30 yr, no single model has yet emerged which can encompass the body of available experimental data. The term "nuclear fog" coined by Siemens[37] with mechanistic connotations, is in many respects an indication of the state of understanding of the responsible process or processes. The present experiment provides evidence that the initial interaction becomes more peripheral as the bombarding energy increases. We emphasize that angular distributions and kinetic quantities derived from them appear to become independent of projectile type and energy and show a reduced dependence on fragment mass at very high energies. These new data are a significant constraint on, and an important clue to developing models for the fragmentation process. Such models must confront an already large body of data from proton induced fragmentation studies and now a rapidly growing body of data from similar investigations that utilize relativistic heavy-ion projectiles. The need is clearly apparent for theoretical approaches which can satisfactorily and simultaneously explain the proton and heavy-ion data in both their simple and more complicated aspects.

This research was carried out at Brookhaven National Laboratory under Contract DE-AC02-76CH00016 with the U.S. Department of Energy and supported by its Office of High Energy and Nuclear Physics.

[1]R. Wolfgang, E. W. Baker, A. A. Caretto, J. B. Cumming, G. Friedlander, and J. Hudis, Phys. Rev. **103**, 394 (1956).
[2]A. I. Warwick, H. H. Wieman, H. H. Gutbrod, M. R. Maier, J. Péter, H. G. Ritter, H. Stelzer, F. Weik, M. Friedman, D. J. Henderson, S. B. Kaufman, E. P. Steinberg, and B. D. Wilkins, Phys. Rev. C **27**, 1083 (1983).
[3]J. Hüfner, Phys. Rep. **125**, 129 (1985).
[4]L. P. Csernai and J. I. Kapusta, Phys. Rep. **131**, 223 (1986).
[5]J. E. Finn, S. Agarwal, A. Bujak, J. Chuang, L. J. Gutay, A. S. Hirsch, R. W. Minich, N. T. Porile, R. P. Scharenberg, B. C. Stringfellow, and F. Turkot, Phys. Rev. Lett. **49**, 1321 (1982).
[6]A. S. Hirsch, A. Bujak, J. E. Finn, L. J. Gutay, R. W. Minich, N. T. Porile, R. P. Scharenberg, B. C. Stringfellow, and F. Turkot, Phys. Rev. C **29**, 508 (1984).
[7]A. L. Goodman, J. I. Kapusta, and A. Z. Mekjian, Phys. Rev. C **30**, 851 (1984).
[8]A. D. Panagiotou, M. W. Curtin, and D. K. Scott, Phys. Rev. C **31**, 55 (1985).
[9]A. Vincentini, G. Jacucci, and V. R. Pandharipande, Phys. Rev. C. **31**, 1783 (1985).
[10]B. V. Jacak, H. Stöcker, and G. D. Westfall, Phys. Rev. C **29**, 1744 (1984).
[11]L. P. Csernai, H. Stöcker, P. R. Subramanian, G. Buchwald, G. Graebner, A. Rosenhauer, J. A. Maruhn, and W. Greiner, Phys. Rev. C **28**, 2001 (1983).
[12]J. Hüfner and H. M. Sommerman, Phys. Rev. C **27**, 2090 (1983); S. Bohrmann, J. Hüfner, and M.C. Nemes, Phys. Lett. **120B**, 59 (1983).
[13]D. R. Fortney and N. T. Proile, Phys. Rev. C **22**, 670 (1980).
[14]L. P. Remsberg and D. G. Perry, Phys. Rev. Lett. **35**, 361 (1975).
[15]D. R. Fortney and N. T. Porile, Phys. Rev. C **21**, 2511 (1980).
[16]N. T. Porile, D. R. Fortney, S. Pandian, R. A. Johns, T. Kaiser, K. Wielgoz, T. S. K. Chang, N. Sugarman, J. A. Urban, D. J. Henderson, S. B. Kaufman, and E. P. Steinberg, Phys. Rev. Lett. **43**, 918 (1979).
[17]R. L. Klobuchar, G. J. Virtes, and J. B. Cumming (unpublished).
[18]Y. Morita, W. Loveland, P. L. McGaughey, and G. T. Seaborg, Phys. Rev. C **26**, 511 (1982); Y. Morita, W. Love-

land, and G. T. Seaborg, *ibid.* **28**, 2519 (1983).
[19]S. B. Kaufman, E. P. Steinberg, and M. W. Weisfield, Phys. Rev. C **18**, 1349 (1978).
[20]S. B. Kaufman, E. P. Steinberg, B. D. Wilkins, and D. J. Henderson, Phys. Rev. C **22**, 1897 (1980).
[21]R. W. Stoenner, W. J. Lyman, and R. Davis, Jr., Geochim. Cosmochim. Acta, Suppl. 1, **2**, 1583 (1970).
[22]R. W. Stoenner, P. E. Haustein, and J. B. Cumming, Phys. Rev. Lett. **53**, 341 (1984).
[23]J. Hudis, T. Kirsten, R. W. Stoenner, and O. A. Schaeffer, Phys. Rev. C **1**, 2019 (1970).
[24]L. P. Remsberg, D. G. Perry, D. Benson, and Y. Y. Chu (unpublished).
[25]S. Pandian and N. T. Porile, Phys. Rev. C **23**, 427 (1981).
[26]G. D. Cole and N. T. Porile, Phys. Rev. C **25**, 244 (1982).
[27]J. B. Cumming, P. E. Haustein, and H.-C. Hseuh, Phys. Rev. C **24**, 2162 (1981).
[28]H. H. Gutbrod, A. I. Warwick, and H. Wieman, Nucl. Phys. **A387**, 177 (1982).
[29]R. E. Renfordt, D. Schall, R. Bock, R. Brockmann, J. W. Harris, A. Sandoval, R. Stock, H. Ströbele, D. Bangert, W. Rauch, G. Odyniec, H. G. Pugh, and L. S. Schroeder, Phys. Rev. Lett. **53**, 763 (1984).
[30]I. Halpern, Nucl. Phys. **11**, 522 (1959).
[31]S. Raha, R. M. Weiner, and J. W. Wheeler, Phys. Rev. Lett. **53**, 138 (1984).
[32]P. Danielewicz, Phys. Lett. **146B**, 168 (1984).
[33]C. B. Chitwood, D. J. Fields, C. K. Gelbke, W. G. Lynch, A. D. Panagiotou, M. B. Tsang, H. Utsunomiya, and W. A. Friedman, Phys. Lett. **131B**, 289 (1983); D. J. Fields, W. G. Lynch, C. B. Chitwood, C. K. Gelbke, M. B. Tsang, H. Utsunomiya, and J. Aichelin, Phys. Rev. C **30**, 1912 (1984).
[34]J. B. Cumming, R. J. Cross, J. Hudis, and A. M. Poskanzer, Phys. Rev. **134**, B167 (1964).
[35]G. D. Westfall, R. G. Sextro, A. M. Poskanzer, A. M. Zebelman, G. W. Butler, and E. K. Hyde, Phys. Rev. C **17**, 1368 (1978).
[36]D. R. Fortney and N. T. Porile, Phys. Rev. C **22**, 670 (1980).
[37]P. J. Siemens, Nucl. Phys. **A428**, 189 (1984).